Biochimica et Biophysica Acta 1808 (2011) 1947–1956

Contents lists available at ScienceDirect

Biochimica et Biophysica Acta

journal homepage: www.elsevier.com/locate/bbamem

Mechanics and dynamics of triglyceride-phospholipid model membranes: Implications for cellular properties and function

Kirsi I. Pakkanen [a,*], Lars Duelund [a], Klaus Qvortrup [b], Jan S. Pedersen [c], John H. Ipsen [a]

[a] MEMPHYS – Center for Biomembrane Physics, Department of Physics and Chemistry, University of Southern Denmark, Odense, Denmark
[b] Department of Biomedical Sciences, University of Copenhagen, Copenhagen, Denmark
[c] Department of Chemistry and iNANO Interdisciplinary Nanoscience Center, University of Aarhus, Aarhus, Denmark

ARTICLE INFO

Article history:
Received 27 September 2010
Received in revised form 10 April 2011
Accepted 11 April 2011
Available online 21 April 2011

Keywords:
Triglyceride
Phospholipid membrane
Membrane conformational dynamics
Membrane mechanics

ABSTRACT

We demonstrate here that triolein alters the mechanical properties of phospholipid membranes and induces extraordinary conformational dynamics. Triolein containing membranes exhibit fluctuations up to size range of 100 μm and with the help of these are e.g. able to squeeze through narrow passages between neighbouring structures. Triolein–phosphatidylcholine membranes were found to have bending rigidity significantly lower than that of corresponding pure phosphatidylcholine membrane. Moreover, the triolein containing membranes were found to be reluctant to fuse, which is in good accordance with larger lamellar distances observed in the TOPOPC membranes. These findings suggest repulsion between adjacent membranes. We provide a comprehensive discussion on the possible explanations for the observed mechanics and dynamics in the TOPOPC system and on their potential cellular implications.

1. Introduction

Triglycerides are built from three fatty acids esterified into the hydroxyl groups of a glycerol molecule. Result of this architecture is a very hydrophobic neutral lipid which forms the basis of many natural oils, such as olive oil. Although triglycerides are also found as components of some cellular membranes, their solubility in phospholipid membranes is rather limited. Lamellar phosphatidylcholine bilayers have been measured to allow partitioning of only about 3–5% of triglyceride into the membrane phase [1,2]. Interestingly, in phosphatidylcholine bilayers containing cholesterol, the solubility of triglycerides has been found to fall almost linearly with the increasing cholesterol concentration [3]. Despite of being minor participants in membranes, triglycerides have been reported to have clear effects on the physical properties of phospholipid membranes. Li et al. described triolein to alter both dynamic properties, such as orientation, and structure of the polar headgroups of the phosholipid bilayer [4]. In our recent work we characterised experimentally effects of triolein (TO) on fluid phosphatidylcholine membranes. We found structures formed by TO-phosphatidylcholine mixture to coexist as three macroscopical phases, a lamellar phase (heavy phase), a dilute vesicular phase (light phase) and an oil phase. While the oil phase was located at the air–water interface, the coexistence of the two membrane phases became evident as they efficiently separated either spontaneously by overnight settling or in centrifugal force field. The two phases were found to be surprisingly similar in terms of TO:phospholipid ratio, but differed with respect to their physical properties [2]. Some of the measured differences, though, were later discussed to potentially originate from differences in partitioning of the used probes [5].

Triglycerides are present in the fluid core of triglyceride-rich lipoproteins, which transport dietary triglycerides in blood circulation (reviewed in e.g. [6]). Aggregates similar to these lipoprotein particles, lipid droplets, are found inside cells. Lipid droplets have a fluid triglyceride-rich core covered by phospholipid monolayer decorated with selected proteins. During the biosynthesis of lipid droplets triglycerides accumulate inside the endoplasmic reticulum (ER) membrane and eventually pinch off as droplets covered by a selected population of ER lipids [7,8]. Lipid droplets, which once were seen only as energy reserves serving the cellular metabolism are nowadays acknowledged as independent organelles, which have multiple roles in cellular homeostasis and function [9].

Interestingly, cancer cells have been found to contain significant amounts of triglycerides in their plasma membrane [10]. In 1988 Mountford and Wright presented a model proposing cancer cell plasma membranes to contain triglyceride-rich domains [10]. Similar domains were also found on the plasma membranes of embryonic stem cells and stimulated lymphocytes [11–13]. The theory was based on ^{1}H NMR evidence on isotropically tumbling triglycerides segregated in intrabilayer domains which did not undergo diffusive lipid exchange with surrounding membrane lipids [10]. In a recent study molecular level support was presented for the mobile lipid domain theory based on simulations on the behaviour of triolein in phosphatidylcholine membranes. In addition to

* Corresponding author at: Department of Micro- and Nanotechnology, Technical University of Denmark, Kgs. Lyngby, Denmark. Tel.: +45 652560; fax: +45 65504048.
E-mail addresses: kipa@nanotech.dtu.dk (K.I. Pakkanen), ipsen@memphys.sdu.dk (J.H. Ipsen).

0005-2736/$ – see front matter © 2011 Elsevier B.V. All rights reserved.
doi:10.1016/j.bbamem.2011.04.006

interfacial localisation, the molecular dynamics study showed triolein to form aggregates, so-called blister domains, inside fluid phosphatidylcholine membranes [5].

In the present study we continued the characterisation of the influence of triolein on phosphatidylcholine membranes, which we and our colleagues have also earlier addressed with both experimental [2] and computational methods [5]. We show on model membrane level how incorporation of triolein changes the conformational dynamics of phospholipid membranes and provide a possible explanation for this behaviour. We will also give some examples on potential biological significance of the behaviour.

2. Experimental

2.1. Materials

Lipid stocks were made in chloroform and fluorophore stocks in methanol, both HPLC grade and purchased from Sigma-Aldrich (St. Louis, MO). Ultra pure (18.2 MΩ/cm) water used for vesicle preparations was purified using a Millipore A10 Academic unit (Millipore corp., Billerica, MA). POPC (1-palmitoyl-2-oleoyl-sn-glycero-3-phosphocholine) was purchased from Avanti Polar Lipids (Alabaster, AL). TO (triolein; cis-9-(octadecenoyl)glycerol) and Triton X-100 were from Sigma-Aldrich. All fluorophores, NBD-PE (N-(7-nitrobenz-2-oxa-1,3-diazol-4-yl)-1,2-dihexadecanoyl-sn-glycero-3-phosphoethanolamine), *N*-Rh-PE (rhodamine B 1,2-dihexadecanoyl-sn-glycero-3-phosphoethanolamine) and $DiIC_{18}$ (1,1′-diocta decyl-3,3,3′,3′-tetramethylindocarbocyanine perchlorate) were from Invitrogen (Carlsbad, CA). Grids used for sample preparation for transmission electron microscopy were from Axlab A/S (Vedbæk, Denmark) and PTA (phosphotungstic acid) used for contrast enhancement from Merck (Whitehouse Station, NJ).

2.2. Preparation of vesicles

All TOPOPC vesicles in used in this study were made by mixing POPC and TO in 9:1 molar ratio. According to our previous results [2] this corresponds to roughly 5 mol% TO incorporated into the membrane. Vesicles denoted as POPC were composed of POPC only. Multilamellar vesicles were prepared using a standard procedure. Shortly, the lipids, and then applicable fluorescent probes, were mixed in chloroform and dried first under N_2 flow and then in vacuum. The samples were stored at −20 °C until used. The samples were freshly hydrated for each experiment by shaking them in a rotary shaker for 30 min at 25 °C. The light and heavy phases of the TO containing vesicles were, when applicable, separated in a bench-top centrifuge (Jouan CR3i, Thermo Scientific, Waltham, MA) as described previously [2].

Small unilamellar vesicles (SUVs) were prepared from the multilamellar vesicles. A microtip sonicator (Misonix Sonicator 3000, Misonic Inc. Farmingdale NY) was used to sonicate the sample for 6 min with alternating cycles 30 s 3 W power and 30 s pause to avoid unnecessary heating of the sample.

2.3. Confocal microscopy

Confocal microscopy was performed using a Zeiss LSM 510 META NLO microscope (Carl Zeiss, Jena, Germany). An excitation wavelength of 543 nm was used for $DiIC_{18}$. The samples were prepared in home-made electroformation cells [14]. The SUVs (see 2.2) were deposited as small droplets on platinum wire electrodes and dried in vacuum. The dried lipids were hydrated with water and the chamber was sealed from below with a large cover glass. For TOPOPC samples alternating current (2 V/10 Hz) was applied for ca. 10 min using a waveform generator (Agilent 33120A, Agilent Technologies, Inc., Santa Clara, CA). The electroformation was monitored with the microscope during the process and, when necessary, current was adjusted to the speed of vesicle formation. However, in all cases voltage was applied only for short periods to the TO containing samples, as longer voltage duration was found to destroy the formed vesicular structures. For POPC a standard electroformation procedure was used [15,16]. Both TOPOPC and POPC vesicles were imaged on the electrodes at room temperature under similar conditions.

2.4. Phase contrast microscopy

For studying hydration and spontaneous structure formation, SUVs were deposited on platinium electrodes used routinely for electroformation of giant unilamellar vesicles. The deposits were allowed to dry in room air for 90 min and after that the membranes were re-hydrated by immersing the electrodes in water in a cuvette. No electroformation was used. The spontaneously formed structures were visualised using a phase contrast microscope (Axiovert S100; Zeiss, Göttingen, Germany) equipped with a 40×/0.60 objective. Growth of the structures was followed for 48 h during which the samples were stored at room temperature (24 °C). The experiment was repeated three times with essentially same results each time.

2.5. Bending elasticity measurements

The bending elasticity measurements were made using giant unilamellar vesicles (GUVs). The GUVs were prepared similar to sample preparation for confocal microscopy (see Section 2.4) except that the GUVs used for the bending elasticity measurements were not attached to electrodes. Vesicle fluctuation was recorded using a phase contrast microscope (Axiovert S100 Zeiss, Göttingen, Germany) with a 40×/0.60 objective and a CCD camera (Sony SSCDC50AP; Sony, New York, NY) able to capture pictures at a rate of 25 frames per second. All the measurements were made at 24 °C, maintained with a water bath circulator (Julabo Labortechnik GmbH, Seelbach, Germany). Only spherical, unilamellar and sufficiently large vesicles were selected for measurements based on visual inspection. Membrane bending elasticities were calculated [17] from recorded vesicle contour fluctuations using a home-made software package. Six representative vesicles were used for each calculation.

2.6. Fluorescence spectroscopy

The effect of triglycerides on lipid mixing was analysed using a fluorescence energy transfer (FRET) assay. The assay is based on dilution of donor–acceptor pairs leading to decrease in the acceptor and increase in the donor fluorescence upon lipid mixing between fluorescent and unlabelled vesicles [18]. Multilamellar vesicles of TOPOPC and POPC were prepared with and without both NBD-PE and *N*-Rh-PE (both 0.2 mol%). The TOPOPC vesicles were separated into light (LF) and heavy (HF) phases [2]. Fluorescence spectra of fluorophore containing vesicles as well as mixtures (1:1 volume ratio) of fluorophore containing vesicles and unlabelled vesicles were measured. To obtain measurements without the participation of the acceptor, Triton X-100 was added to mixture of fluorescent and unlabelled vesicles to final concentration of 2 vol.%. Addition of Triton X-100 leads to complete segregation of the donor–acceptor pairs (most likely in micelles) and energy transfer to the acceptor becomes negligibly small. The samples were measured using either an SLM Aminco 8100 fluorometer (SLM Instruments, Urbana, IL) or a Chronos ISS fluorometer (ISS, Champaign, IL). With SLM Aminco both excitation and emission slits were set to 8 nm, whereas with the Chronos ISS slits of 2 nm were used for both. Polarisers at 0° and 90° for excitation and emission, respectively, were used to cut down scattering. The samples were excited at 470 nm. Fluorescence emission was gathered at 490–650 nm. The measurements were made at 25 °C, which was maintained with a water bath circulator (Julabo Labortechnik GmbH, Seelbach, Germany). Triton affects the emission intensities of fluorophores [19] and it was therefore necessary to correct the emission intensities at NBD-PE's emission maximum (530 nm) as these values

were used in the energy transfer efficiency calculations. As fluorophores may act differently on TO containing membranes [5], correction factors were measured independently for the pure POPC system and the TO containing system. Fluorescence resonance energy transfer efficiency was calculated from the obtained intensity values using equation:

$$E = 1 - \frac{F}{F_0} \quad (1)$$

where F is the fluorescence emission intensity of the donor (at 530 nm) in the absence and F_0 in the presence of Triton [18]. The calculated energy transfer efficiencies were normalised to the case of optimal energy transfer, i.e. in the absence of unlabelled vesicles. Each measurement was repeated three times in parallel. Numbers presented are mean of six independent samples.

2.7. Differential scanning calorimetry

A TA instruments Nano DSC (TA instruments, Lindon, UT) was used for DSC measurements. Mixing of lipid between TOPOPC and POPC membranes with DPPC membranes was investigated by mixing equal volumes of 5 mM DPPC multilamellar vesicles with 5 mM TOPOPC, POPC or DPPC (control) multilamellar vesicles. The mixtures were scanned from 25 °C to 50 °C with a scan rate of 0.5 °C/min for minimum of 7 times (upscans). The main phase transition peak positions and the peak onset temperature (T_{onset}) were determined using the Nanoanalyze program (TA instruments). The presented numbers are mean of six independent measurements.

2.8. Transmission electron microscopy

Multilamellar vesicles were used for transmission electron microscopy (TEM). Vesicles were mixed in 1:1 volume ratio with 2% PTA (pH 7.0) and dried on grids at room temperature. Following drying, the samples were imaged immediately using a Philips CM 100 transmission electron microscope (Philips, Eindhoven, The Netherlands) operated at an accelerating voltage of 80 kV. Digital images were obtained with a MegaView II camera and the analySIS software package (Soft Imaging Systems, Münster, Germany). Distance between lamellae was measured from the TEM micrographs. Artefacts and background noise were subtracted from images by Fourier transform filtering and grey values for each pixel on a line drawn over a set of bilayers were plotted against distance on the line. The difference in distance between succeeding local minima of grey values was calculated from this data. The local minima correspond to the dark pixels in the picture, which represent the lipid bilayers labelled with PTA. Image analysis was made using the ImageJ software [20]. Four images were analysed for each data set, 4 to 6 calculations (each containing 3 to 12 lamellae) were made in each image.

2.9. Small-angle X-ray scattering

Small-angle X-ray scattering experiments (SAXS) were performed on the prototype of the commercially available NanoStar camera (Bruker AXS) located at Aarhus University [21]. The instrument uses a rotating anode source (Cu K-alpha) and a pair of Göbel multilayer mirrors in Montell geometry. The beam is collimated by three pinholes and the scattering is recorded by a position-sensitive gas proportional counter (HiSTAR, Bruker AXS). The instrument is optimised for solution scattering, has an integrated vacuum and employs a semi-transparent beamstop for beam monitoring. The intensity is recorded as a function of the modulus of the scattering vector:

$$q = 4\pi \ sin(\theta) / \lambda \quad (2)$$

where λ is the X-ray wavelength and θ is half the scattering angle. The sample is measured in a reusable quartz capillary sealed with steel caps and o-rings. The temperature was 25 °C and controlled by placing the capillary in a thermostated block. Water was measured as a background in the same capillary. The recorded intensities were azimuthally averaged and the water signal was subtracted from the signal from the sample. The SAXS data was analysed using the full-profile modelling approach by Pabst et al. [22] for multilamellar stacks of bilayers. In this approach the cross-section of the bilayers is described by three Gaussian functions, one for the central hydrocarbon region and two placed symmetrically for the lipid headgroups. The correlation between the layers is described by the modified Caille theory [23,24] in terms of a structure factor. The scattering of the sample is assumed to be given by the sum of the scattering from the bilayers and that of single bilayers. The model was implemented in a home-written least-squares program [25] and polydispersity of the number of layers in the multilamellar stacks was included (C.L.P. Oliveira and J.S. Pedersen, unpublished). The instrumental resolution function that leads to a smearing of the recorded intensities was estimated from the parameters of experimental setup and smearing was included in the modelling by numerically convolving the model intensities by the resolution function. [26,27]. The results comprise 2–4 individual measurements.

2.10. Statistics

Pair-wise statistical testing was performed using the non-parametric Mann–Whitney U test. Confidence level was set to 0.05. Statistical analyses were made using R [28].

3. Results

3.1. Structure formation and dynamics

In a recent study TO was found in phospholipid membranes to be for the most part positioned into an interlamellar oil-phase, a blister domain, inside the lipid bilayer using molecular dynamics simulations [5]. Such abnormal localisation of triglycerides could have dramatic effects on the morphology and behaviour of the TO containing membranes. To learn more about structure formation and morphology in the TOPOPC system we used microscopy to look closer into the formed structures.

3.1.1. Confocal microscopy

We used confocal microscopy to visualise the morphology of TO containing membranes. During these experiments we found that the dynamics of the vesicular structures formed by the TOPOPC system differ clearly from those normally seen with pure phospholipids or different binary and ternary mixtures (see e.g. [16,17,29]). Firstly, the normal electroformation protocol routinely used to form GUVs for phospholipids in water [15,16] did not work for the TOPOPC mixture. Instead of GUVs a mesh of tubular structures with some vesicular parts and collapsed lipid masses was formed (data not shown). Through empirical optimisation we learned that large vesicular structures, among them also GUVs, can with TOPOPC only be formed using very short electroformation times. Where the electroformation of phospholipids has duration in the order of hours, was the time to form TOPOPC GUVs in the order of minutes. Even then, the system forms a very heterogenious mixture of structures ranging from tubules to multi- and unilamellar vesicles (see Fig. 1). All the formed structures were homogeneously labelled with the probe $DiIC_{18}$ and no preference for the probe to partition into domains could be seen (Fig. 1). GUVs composed of POPC only were produced by normal electroformation procedure and, as expected, showed as well homogeneous labelling with $DiIC_{18}$ (Fig. 2). The most striking finding in the confocal microscopy study was not the morphology or labelling but the mobility of the TOPOPC structures. Unlike the close to stationary POPC vesicles, a large portion of the TOPOPC structures experienced drastic and rapid alterations in their conformation. The TOPOPC membranes were in the form of tubules in a reptation-like

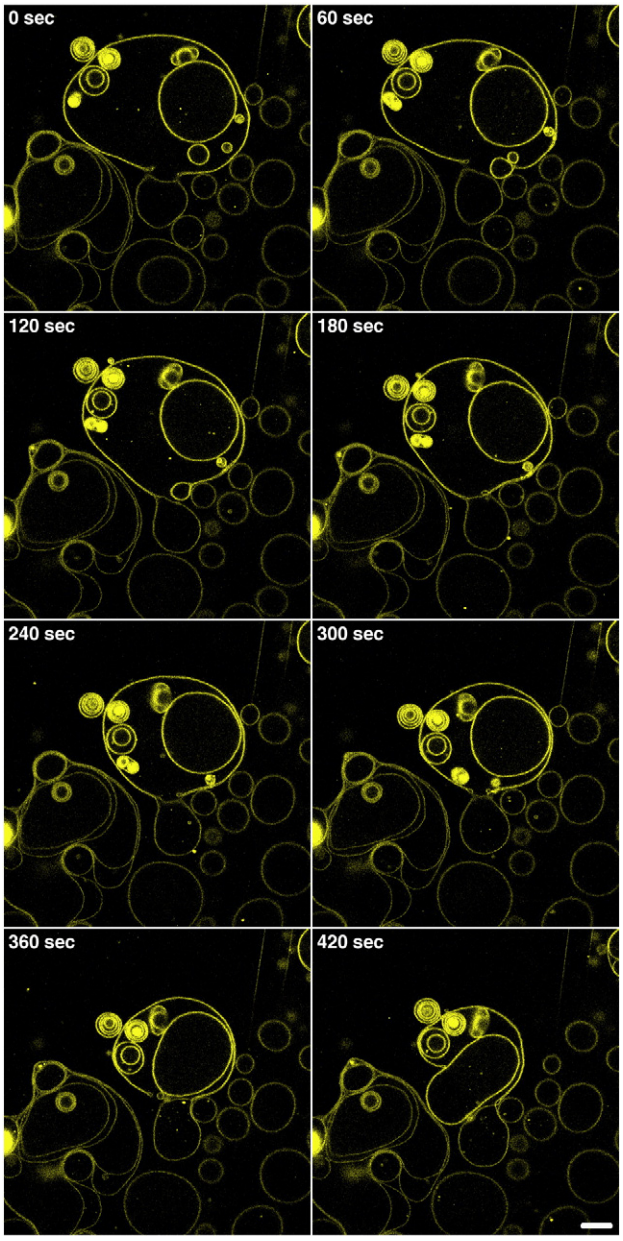

Fig. 1. A time series (0 to 420 s) visualising the movement of TOPOPC structures labelled with $DiIC_{18}$. Bar 20 μm applies to all time points in the series.

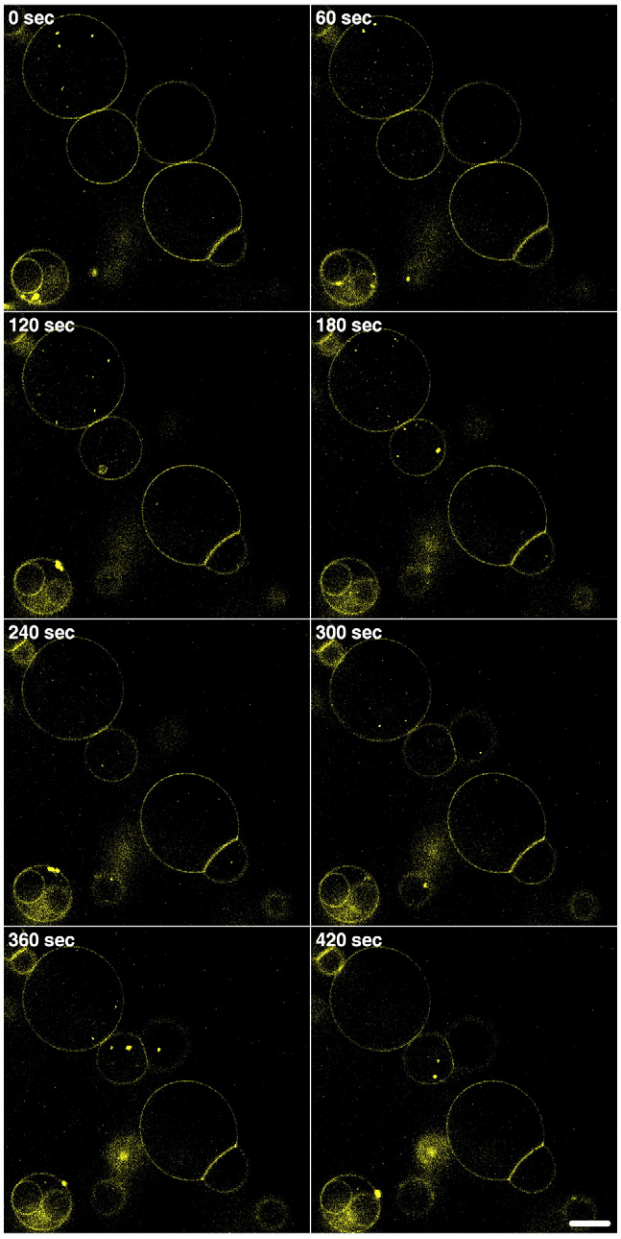

Fig. 2. A time series (0 to 420 s) of POPC structures labelled with $DiIC_{18}$. Bar 20 μm applies to all time points in the series.

motion, whereas the vesicular structures were seen to experience strong long wavelength fluctuations in the length scale of 100 μm and to squeeze between the neighbouring structures while diffusing forward (Figs. 1 and 2; Supplementary material, Films 1 and 2 for TOPOPC and POPC, respectively).

3.1.2. Phase contrast microscopy

The abnormal behaviour observed with electroformation of the TOPOPC mixture prompted us to study closer the way these membrane structures are formed. No electroformation was used to form the structures in this experiment but they were allowed to develop spontaneously. Marked differences were seen in the behaviour of the TOPOPC mixture and pure POPC. The initial hydration of TOPOPC membranes appeared to be faster in general. In addition, succession of different types of structures seemed to proceed at a somewhat higher speed. Already at 5 min after hydration TOPOPC had formed multilamellar structures of considerable size whereas pure POPC presented mainly short protruding tubular structures and semicircular unilamellar structures lying on the support (Fig. 3 (5 min)). At 15 min vesicular structures, seemingly uni- or oligolamellar, dominated in the POPC sample (Fig. 3 (15 min)). In TOPOPC sample the initial looser multilamellar structures had evolved into predominantly thick elongated multilamellar structures. Free volume inside the structures (if they indeed were closed) seemed to be much smaller than the volume occupied by the thick bundles of lamellae (Fig. 3 (15 min)). POPC begun to show signs of multilamellarity at 30 min. At that point the typical scenery of thick lamellar bundles of TOPOPC had already started to evolve towards more typical multilamellar structures, which also were getting a more vesicular configuration (Fig. 3 (30 min)). By 60 min the POPC structures had reached a significant degree of multilamellarity, thus catching up on the TOPOPC structures which already at 5 min had showed initial signs of multilamellarity (Fig. 3 (60 min)). At 24 h the POPC sample had not changed much from that at 1 h: classically onion-like multilamellar vesicles were the most prominent structures in view,

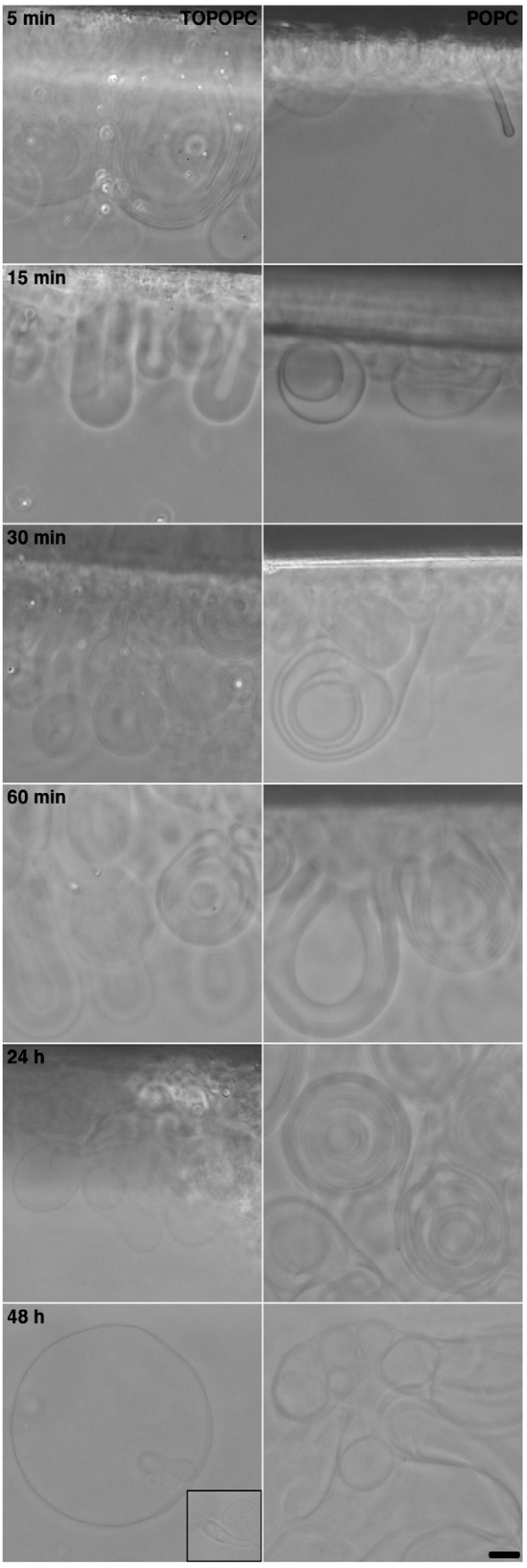

Fig. 3. Hydration of TOPOPC (left panel) and POPC (right panel) into spontaneously formed structures. Time points refer to time after addition of water into the system. Snapshots represent typical structures seen in the observation cuvette. Inset in the picture TOPOPC at 48 h represents the other typical structure seen in the system. The pictures are a representative series from one of the three individual experiments made. Bar 10 μm.

although in some the multilamellarity seemed less pronounced. The TOPOPC structures had experienced some drastic changes when observed at 24 h. The multilamellar structures had collapsed into unilamellar vesicular and tubular structures. In addition, some more dense collapsed material was visible (Fig. 3 (24 h)). 24 h later, at 48 h after addition of water, seemingly free standing unilamellar vesicles of respectable size had appeared in the cuvette containing TOPOPC. Along with them coexisted also a heterogenious collection of multivesicular structures, some of them connected or tethered by thin membrane tubes. Also with POPC the situation had changed since the 24 h time point. Majority of the multilamellar vesicles had disappeared and the dominating structures seemed to be folded membrane stacks with some vesicular and some lamellar regions. Some smaller unilamellar vesicles were to be found. (Fig. 3 (48 h)).

3.2. Bending elasticity

Mechanical properties of membranes are critical nominators of their properties. We investigated the mechanics of the TOPOPC system using vesicle fluctuation analysis and calculated the bending elasticity for the membranes. Compared to pure POPC for which the bending elasticity was calculated to be $1.46 \cdot 10^{-19}$ J, the TOPOPC membrane was found to be extremely soft. The bending elasticity of TOPOPC membranes was close to being only third of that of POPC's, $0.66 \cdot 10^{-19}$ J. Difference in bending elasticities between pure POPC and TOPOPC was found to be statistically significant ($P = 0.0048$).

3.3. Lipid mixing

To better understand the unique behaviour of the TOPOPC system we wanted to investigate whether the membranes are more susceptible to lipid mixing than pure POPC membranes. We studied the matter with two different approaches. To find out to what extent TOPOPC membranes are able to exchange lipids with membranes of the same composition we used a fluorescence resonance energy transfer (FRET) assay described by Struck et al. [18]. Mixing of lipids between TOPOPC membranes and DPPC membranes was studied with differential scanning calorimetry (DSC) similar to the approach used by Higashino et al. [30].

3.3.1. Fluorescence energy transfer

The FRET assay used here to study lipid mixing is based on dilution of the donor–acceptor pairs upon mixing of lipids between fluorescent and unlabelled vesicles [18]. As fluorescence based methods are sensitive and not dependent on the absolute lipid amount in the sample we were able to analyse lipid mixing in both light and heavy phase (described in [2]) separately. Fluorescent spectra of vesicles containing both donor (NBD-PE) and acceptor (*N*-Rh-PE) were measured with and without addition of unlabelled vesicles. In the end of each measurement Triton X-100 was added. In general terms spectra measured with fluorescent vesicles, either with or without added unlabelled vesicles, featured two emission maxima, the first at 530 nm by NBD-PE and the second at 585 nm by *N*-Rh-PE. The emission of *N*-Rh-PE originated for the most part from energy transfer from NBD-PE and, correspondingly, the Rh emission maxima have higher intensities than the NBD maxima. The Rh emission maxima intensities of the spectra measured with added unlabelled vesicles were somewhat lower than of the spectra measured without added unlabelled vesicles. This arises from slightly lowered ability for the

NBD to transfer energy to Rh caused by dilution of the FRET pairs. In the spectra measured after addition of Triton X-100 the Rh emission peak had almost disappeared as the FRET pairs became separated from each other. Equivalent increase in NBD emission intensity was also observed, as its energy was now used for fluorescence instead of excitation of Rh through energy transfer (Fig. 4A–C).

The decrease in the emission intensity of the energy transfer excited Rh was quantified by calculating energy transfer efficiency (Eq. 1). The energy transfer efficiency is inversely correlated to the amount of lipid mixing, between the fluorescent and unlabelled vesicles. The calculated efficiencies were normalised to the optimal energy transfer efficiencies, i.e. the case without unlabelled vesicles where no lipid mixing could be detected. For POPC the calculated energy transfer efficiency was 91% (SE (standard error) 4%) which tells that only a small fraction of the fluorescent POPC vesicles to have fused with the unlabelled POPC vesicles. For TOPOPC HF the energy transfer efficiency was calculated to be slightly higher, 98% (SE 2%). Even higher the number was for TOPOPC LF, 102% (SE: 5%; Fig. 4D). The differences in the energy transfer efficiencies between the TO containing membranes and pure POPC were small and not statistically significant. However, based on the results we can say that in the short time scale of observation used here TOPOPC membranes, neither the heavy (HF) and the light (LF) phase have increased ability to exchange lipids with membranes of equal composition when compared with pure POPC membranes.

3.3.2. Differential scanning calorimetry

To support and elaborate the results acquired using the FRET assay, we also studied membrane lipid mixing in the TOPOPC system using differential scanning calorimetry. Although rarely seen in lipid mixing studies, DSC is an efficient tool to analyse the extent of lipid mixing in heterotypic systems [30]. We selected DPPC to be the mixing partner in our study. In the study, pre-formed TOPOPC or POPC multilamellar vesicles were mixed with DPPC multilamellar vesicles and the mixture was heated over the DPPC main phase transition. Changes in the acquired thermograms were then analysed to obtain information on lipid mixing. The overall form of all the obtained thermograms resembled closely those measured with pure DPPC only (Fig. 5A). When DPPC vesicles were mixed with TOPOPC vesicles, or in particular POPC vesicles, some minute alterations in the thermograms were visible. Modest depressions in the peak temperatures were noticeable but most importantly the transition peak was slightly broadened towards lower temperatures caused by addition of impurities (POPC, TO or both) into the DPPC membrane through lipid mixing between the vesicles. This change was quantified by extracting peak onset temperatures (ΔT_{onset}) from the data (Fig. 5B).

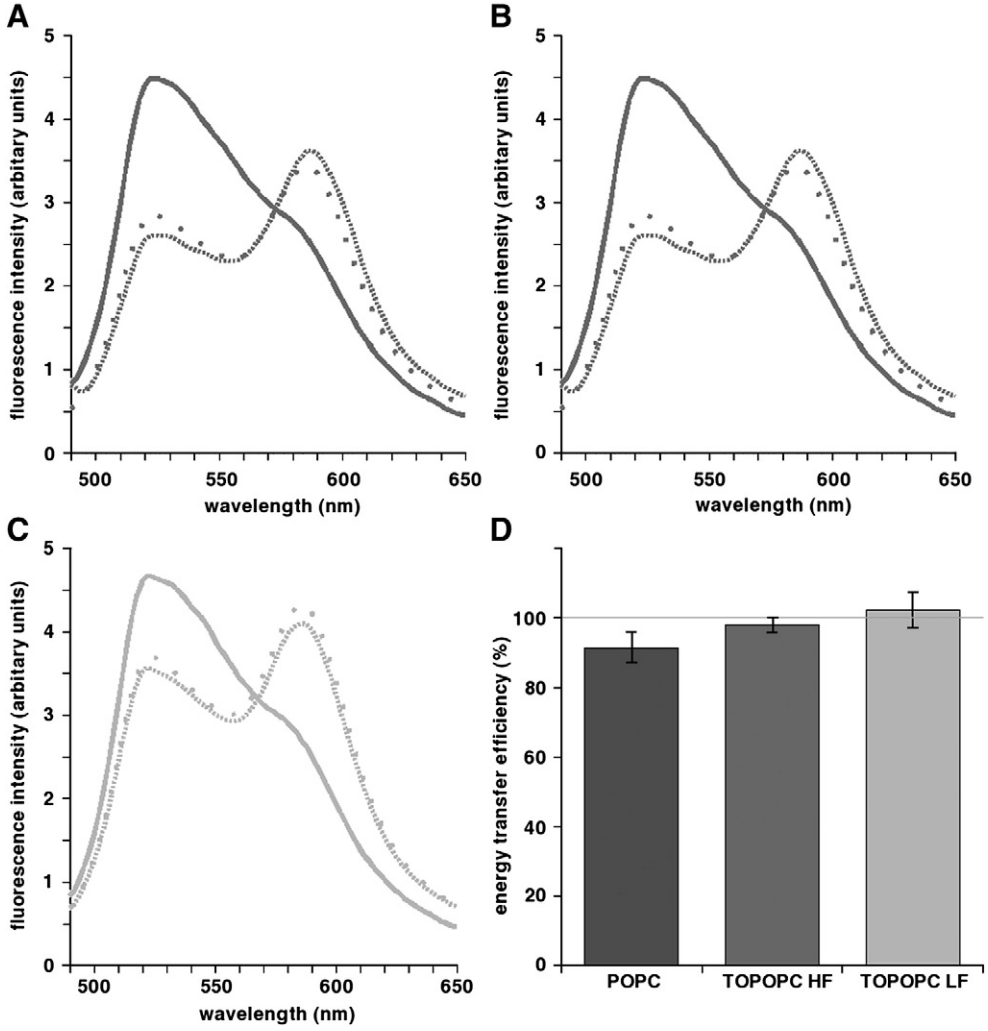

Fig. 4. FRET assay for lipid mixing. Spectra of pure POPC (A), TOPOPC HF (B) and TOPOPC LF (C) show representative spectra measured without unlabelled vesicles (• • •), with unlabelled vesicles (— — —) and with Triton X-100 added (——). Calculated energy transfer efficiencies normalised to optimal energy transfer for each system (100%) (D). Error bars represent SE.

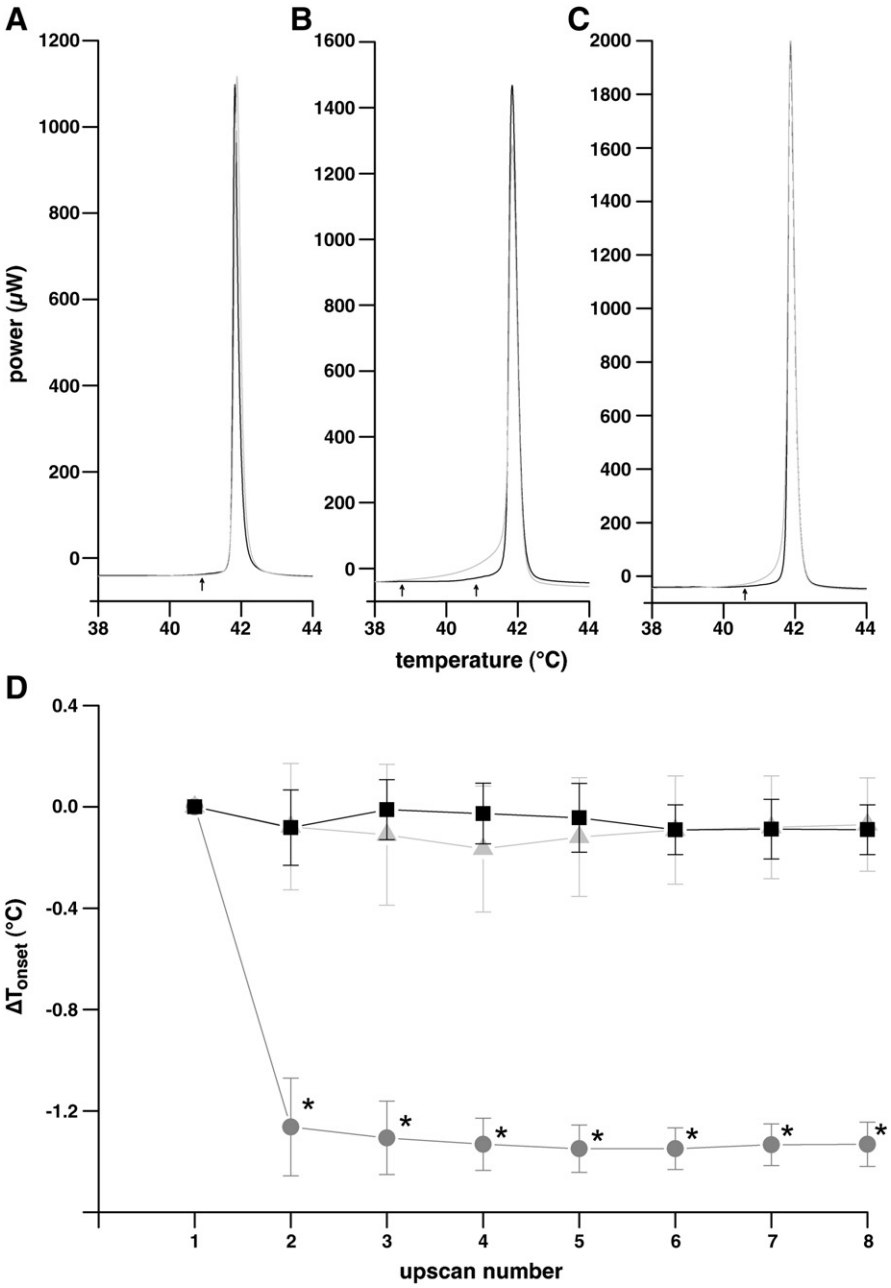

Fig. 5. Lipid mixing studied using differential scanning calorimetry. Thermograms of the first (black line) and seventh (grey line) upscans of DPPC mixed with either DPPC vesicles (A), POPC vesicles (B) or TOPOPC vesicles (C). Differences in the peak onset temperature, ΔT_{onset} (marked with arrows; for more details see section "Experimental") as a function of scan number (D). Colour key: DPPC vesicles mixed with: DPPC vesicles (black), POPC vesicles (dark grey) or TOPOPC vesicles (light grey). Only upscan ΔT_{onset}s are shown, the lines between dots are only guide to the eye. Error bars represent SE. Asterisk shows statistical significance, $P<0.05$.

For control case, DPPC mixed with DPPC, T_{onset} stayed, as expected, unchanged during seven upscans. TOPOPC, when mixed with DPPC vesicles, followed for the most part the unaltered pattern of the DPPC control, but a small change was seen in the case of POPC. By the second upscan (scan nr. 3) the T_{onset} had decreased 1.3 °C. After this drop, the ΔT_{onset} remained stabile and did not decrease further during the following six upscans. Statistical testing revealed the peak onset temperatures of upscans 2–7 for POPC mixed with DPPC vesicles to be significantly different from the corresponding upscans of DPPC only and TOPOPC mixed with DPPC ($P=0.029$ for each). When in a control measurement POPC and DPPC were incorporated into the membrane in a 1:1 molar ratio, the system was observed to undergo a broad phase transition starting from −4 °C. The ΔT_{onset} was 45 °C, which is in good accordance with the DPPC/POPC phase diagram published earlier [31]. The phase diagram shows the ΔT_{onset} to be constant between 0 and 75 mol% and increase linearly between 75 and 100 mol% DPPC. The information extracted from the phase diagram allows us to estimate the amount of POPC incorporated into the DPPC membranes in the lipid mixing experiment to be in the order of 0.7 mol% where for the TO containing membranes the number was negligibly small.

3.4. Distance between lamellae

The distance between lamellae, lamellar repeat distance, was measured using SAXS. Small but clear difference in the distance between the hydrated lamellae for TOPOPC and POPC was measured. The measured lamellar repeat distance was slightly higher for the TO

containing membranes than for pure POPC and in the case of LF the difference was found significant. For TOPOPC HF lamellar repeat distance was measured 6.5 nm, for TOPOPC LF 6.6 nm ($P = 0.065$) and for pure POPC 6.4 nm. The SAXS results suggest multilamellar bilayers in TOPOPC structures to be further apart than the lamellae in POPC structures (Supplementary material Fig. 1).

4. Discussion

In this paper we have in a series of experiments demonstrated the unique conformational dynamics induced by TO in phospholipid membranes and provided some experimental evidence to clarify background for the behaviour. To our knowledge this is the first time such rapid large scale motion as seen now with TO containing membranes (Fig. 1; Supplementary Film 1) is reported to be observed in model membranes. In simple terms, the motion seen in the membranes containing TO can be described as large scale long wavelength fluctuations, which allow the structures to change shape with a surprising speed resulting in spontaneous movement of the structures with respect to each other.

There are three key factors for the characteristics of membrane dynamics: membrane elasticity, the modes of molecular motion of membrane components and the energy dissipation mechanisms involved. Khandelia et al. [5] demonstrated that triglycerides can adopt three major positions in POPC membranes. They can appear in an interfacial state, in a mid-membrane state and at higher triglyceride concentrations (~2%) segregate into blister domains in the hydrophobic core of the membrane. In addition, the study showed that the exchanges of triglycerides between these positions are fast, in the range of milliseconds [5]. All these properties are important ingredients to the above mentioned factors.

In the present study membrane elasticity was characterised using vesicle fluctuation analysis, where the bending elasticity of TOPOPC membranes was found to be strongly reduced compared to POPC membranes. This is interesting as the TOPOPC membranes do not seem to be less ordered than POPC membranes [5]. Instead of chain order alterations, the increased ability of TO molecules to change bilayer leaflet could contribute to the softness of the membrane through direct lowering of the energy to bend the membrane by the mechanism suggested by Leibler [32].

The molecular motions in the TOPOPC membranes also differ significantly from pure phosphatidylcholine membranes, where the lipids are confined to the monolayer leaflets on the time scale of hours. For the TOPOPC membrane rapid exchange of material between the phospholipid monolayers and possible triglyceride blister domains alter the dynamical description of the membrane dramatically. For phosphatidylcholine membranes the only relevant energy dissipation mechanisms for shape dynamics seem to be the viscous friction of the embedding solvent and the intermonolayer friction, where the latter is dominating in long time scales [33,34]. The presence of triglycerides in the mid-plane of the bilayer may serve as a lubricant for the brushing motion of the two membrane leaflets against each other. A detailed theoretical analysis of the effects from the energy dissipation due to the fast triglyceride flip-flop is required to understand the system better.

In addition to rapid shape dynamics the TOPOPC membranes exhibited fast and dynamic structure formation when dehydrated membranes were re-hydrated in a time follow experiment (Fig. 3). Rapid creation of vesicular structures was also demonstrated by difficulties in formation of GUVs by electroformation technique. TOPOPC membranes did not tolerate the normal electroformation protocol used routinely for POPC [15,16], but required ten times shorter exposure to voltage to yield spherical unilamellar vesicles (data not shown). The fast hydration of TOPOPC could arise from increased steric entropic repulsion, due to the decreased bending stiffness [35], and the altered membrane dynamics. Our present results on bilayer distances in multilamellar structures also suggested repulsion between bilayers in the TOPOPC system. Repulsion may also be deduced as background for TO's ability to diminish packing of collapsed membrane lamellae during dehydration as suggested by electron micrographs (Supplementary material Fig. 1). In addition to the steric entropic repulsion, the interbilayer triglyceride blister domains [5] can offer some background for the repulsion by direct local thickening of the membrane.

With two different approaches to lipid mixing, one investigating mixing between membranes of equal composition, one investigating the process between membranes of different composition, we found that the fusogenicity of the TOPOPC membranes did not contribute to its fast hydration (Fig. 4, 5), which again could arise from interbilayer repulsion. The high energy transfer efficiencies – that is to say low lipid mixing ability – seen for the TO system, are likely not to arise from artefacts caused by anomalous partitioning of the probes, as suggested recently [5] concerning previous fluorescence measurements with the TOPOPC system [2]. The probes used in the lipid mixing measurements in the present study, NBD-PE and *N*-Rh-PE, both carry a net charge and are therefore most likely anchored to the membrane–water interphase.

To make biophysics matter more in the biological world, one has to make a jump from simplified models to Nature's full complexity. Although reduced to minimum in terms of components, and thus interactions, model membrane studies give a clear insight into how different lipids contribute to the ensemble properties of natural membranes. In the present study we have elucidated the role of a triglyceride, triolein (TO), on fluid phospholipid membranes. The present study is continuance to our and our colleagues' previous efforts to understand the physical properties of triglyceride containing membranes and through that the biological significance of triglycerides as membrane components. We describe in this work how the TO containing membranes exhibit unique dynamics and discuss how this behaviour could be dictated by altered mechanical properties and organisation of the membrane. It is clear that such drastic changes in a membrane as those induced by triglycerides will have significance also for properties of cells and membrane-associated cellular functions.

Triglycerides have classically not been considered as significant components of biological membranes, and interest in their role in biology has been focused largely on non-bilayer systems such as lipoprotein particles and lipid droplets, formed by a neutral lipid core typically rich in triglycerides covered by a monolayer of phospholipids and free cholesterol, supplemented in the case of lipid droplets by lysolipids [36,37]. Lipid droplets are formed on the endoplasmic reticulum (ER) where neutral lipids are assumed to accumulate between the leaflets of the ER membrane. How these nascent lipid droplets growing in size eventually bud from the parent membrane is not known. Similarly, the fusion abilities lipid droplets with either ER or other membranes or with each other are so far only poorly characterised [7,38]. Our present results suggest that triglycerides inside the membrane could directly influence these processes either by softening the parent membrane in general or inducing a localised softening effect on the area where triglycerides aggregate inside the membrane. The latter possibility is particularly interesting as lipid droplets have been suggested to form in specialised ER membrane subdomains with a particular lipid composition [39,40], which could be preferentially influenced by the softening effect of triglycerides found in our study.

Similarly could a local perturbation in the mechanical properties and dynamic behaviour of membranes have a facilitating or even regulating influence on the function of other intracellular organelles containing triglycerides. Lysosomes have been reported to contain triglycerides [41–43], which is not surprising as lysosomes are the end-station for lipoprotein particle tracking, to which lipoprotein particle lipids are transported after particle dismantling in earlier structures of the endosomal system [44]. Similarly, ER, the site for triglyceride biosynthesis and lipid droplet formation [7,8], is rich is triglycerides [45].

Certain cell types contain significantly more triglycerides than others. Human peripheral blood lymphocytes have been found to contain as

much as 491 nmol triglycerides per mg total lipid and several cancer lines up to ca. 90 nmol triglyceride/mg lipid [11]. Despite several lines of evidence [10,46–48], the "mobile lipid domain" model, where triglycerides are suggested to reside between the two leaflets of cancer cell plasma membranes [10], has attracted criticism since it's appearance. In particular, the lack of physical verification hindered it gaining widespread acknowledgement [49–52]. Some 20 years after the model was proposed clear physical evidence and legitimation, although indirectly, to intramembrane triglyceride-rich domains was provided by showing that in phospholipid membranes triglycerides aggregate spontaneously into blister domains between the two monolayers of the membrane [5]. With this strong support we see the theory for the mobile lipid domains – corresponding to the blister domains – to exist on plasma membranes of cancer and embryonic cells as well as stimulated lymphocytes acceptable. In our present study we demonstrate the effect of such domains on the physical properties of phospholipid membranes. Similar alterations in membrane properties are likely to be induced in plasma membranes where triglyceride blister domains are present.

Accepting the presence of triglyceride blister domains in plasma membranes of these cells links triglycerides to physical properties of cell plasma membranes, cancer cells' in particular, and provides a new viewpoint e.g. into connection between plasma membrane properties and cellular movement. Many of the cell types moving with amoeboid strategy i.e. squeezing through small openings in the ECM [53,54], have been found to have triglycerides located in their plasma membrane [11–13,55] presumably organised as blister domains. In addition, metastatic potential of cancer cells, which is intimately connected with motility [56], has been proposed to be mediated by mobile lipid domains (i.e. triglyceride blister domains) shed by metastatic cancer cells and absorbed by others [10,57–59].

In the present study we found triglycerides, which are likely to reside, at least partly, in blister domains in model phospholipid membranes, to make the membrane unusually soft, having less than half of the bending stiffness of a fluid phospholipid membrane. In addition, triglycerides were also found to enhance membrane–membrane repulsion mediated by large fluctuations arising from the low bending stiffness, and the membranes were found to undergo spectacular spontaneous changes in vesicle conformation. Although cytoskeleton has a crucial role in cellular movement (for review see e.g. [60]), are dramatic alterations in the cell plasma membrane mechanics and dynamics, such as those seen in the present study with triglycerides in phospholipid membranes, potent facilitators of cellular movement by easing the cytoskeleton-dependent formation of plasma membrane protrusions. To extend a membrane hemisphere, a rough model for the leading edge of a moving cell, through a hole into a vacant space on the other side, the energy needed is: $\Delta E = 4\pi\kappa$. Softening of by triglycerides will thus lower significantly the energy required for plasma membrane deformation, as the energy for the deformation is directly proportional to the bending elastic modulus, κ.

In summary, our present study points out some fundamental general differences between pure phosphatidylcholine (POPC) bilayers and bilayers containing TO. We demonstrated here how triolein induces unique alterations in the mechanical properties of phosphatidylcholine membranes as well as extraordinary conformational dynamics. This, as well as the observed reluctancy of TO containing POPC membranes for lipid mixing with other membranes is likely to have significance in the biological world as discussed earlier and provide thus a starting point for further studies on the role of triglycerides in the structure and function of cellular membranes.

Supplementary materials related to this article can be found online at doi:10.1016/j.bbamem.2011.04.006.

Acknowledgements

The authors thank Mary-Ann Gleie (University of Copenhagen, Denmark) and Manja A. Behrens (University of Aarhus, Denmark) for their skilled assistance. Himanshu Khandelia (University of Southern Denmark, Denmark) is thanked for insightful comments on the manuscript. MEMPHYS – Center for Biomembrane Physics is supported by the Danish National Research Foundation.

References

[1] J.A. Hamilton, Interactions of triglycerides with phospholipids: incorporation into the bilayer structure and formation of emulsions, Biochemistry 28 (1989) 2514–2520.
[2] K.I. Pakkanen, L. Duelund, M. Vuento, J.H. Ipsen, Phase coexistence in a triolein–phosphatidylcholine system. Implications for lysosomal membrane properties. Chem Phys Lipids 163 (2010) 218–227.
[3] P.J.R. Spooner, D.M. Small, Effect of free cholesterol on incorporation of triolein in phospholipid bilayers, Biochemistry 26 (1987) 5820–5825.
[4] K.-L. Li, C.A. Tihal, M. Guo, R.E. Stark, Multinuclear and magic-angle spinning NMR investigations of molecular organization in phospholipid-triglyceride aqueous dispersions, Biochemistry 32 (1993) 9926–9935.
[5] H. Khandelia, L. Duelund, K.I. Pakkanen, J.H. Ipsen, Triglyceride blisters in lipid bilayers: implications for lipid droplet biogenesis and the mobile lipid signal in cancer cell membranes, PLoS One 5 (2010) e12811.
[6] J. Heeren, U. Beisiegel, Intracellular metabolism of triglyceride-rich lipoproteins, Curr Opin Lipidol 12 (2001) 255–260.
[7] D.J. Murphy, J. Vance, Mechanisms of lipid-body formation, Trends Biochem Sci 24 (1999) 109–115.
[8] H.L. Ploegh, A lipid-based model for the creation of an escape hatch from the endoplasmic reticulum, Nature 448 (2007) 435–438.
[9] S. Martin, R.G. Parton, Lipid droplets: a unified view of a dynamic organelle, Nat Rev Mol Cell Biol 7 (2006) 373–378.
[10] C.E. Mountford, L.C. Wright, Organization of lipids in the plasma membranes of malignant and stimulated cells: a new model, Trends Biochem Sci 13 (1988) 172–177.
[11] G.L. May, L.C. Wright, K.T. Holmes, P.G. Williams, I.C.P. Smith, P.E. Wright, R.M. Fox, C.E. Mountford, Assignment of methylene proton resonances in NMR spectra of embryonic and transformed cells to plasma membrane triglyceride, J Biol Chem 261 (1986) 3048–3053.
[12] A.J. Dingley, N.J. King, G.F. King, An NMR investigation of the changes in plasma membrane triglyceride and phospholipid precursors during the activation of T-lymphocytes, Biochemistry 31 (1992) 9098–9106.
[13] M.F. Veale, A.J. Dingley, G.F. King, N.J. King, ^{1}H-NMR visible neutral lipids in activated T lymphocytes: relationship to phosphatidylcholine cycling, Biochem Biophys Acta 1303 (1996) 215–221.
[14] M. Fidorra, L. Duelund, C. Leidy, A.C. Simonsen, L.A. Bagatolli, Absence of fluid-ordered/fluid-disordered phase coexistence in Ceramide/POPC mixtures containing cholesterol, Biophys J 90 (2006) 4437–4451.
[15] M.I. Angelova, D.S. Dimitrov, Liposome electroformation, Faraday Discuss Chem Soc 81 (1986) 303–311.
[16] M.I. Angelova, S.Soléau, P.Méléard, F.Faucon, P.Bothorel, Preparation of giant vesicles by external AC electric fields. Kinetics and applications, volume 89 of Progress in Colloid and Polymer Science, Springer Berlin / Heidelberg, pp. 127–131.
[17] J. Henriksen, A. Rowat, J. Ipsen, Vesicle fluctuation analysis of the effects of sterols on membrane bending rigidity, Eur Biophys J 33 (2004) 732–741.
[18] D.K. Struck, D. Hoekstra, R.E. Pagano, Use of resonance energy transfer to monitor membrane fusion, Biochemistry 20 (1981) 4093–4099.
[19] J.R. Silvius, R. Leventis, P.M. Brown, M. Zuckermann, Novel fluorescent phospholipids for assays of lipid mixing between membranes, Biochemistry 26 (1987) 4279–4287.
[20] W. Rasband, U.S. ImageJ, National Institutes of Health, Bethesda, Maryland, USA, 1997–2005, http://rsb.info.nih.gov/ij/
[21] J.S. Pedersen, A flux- and background-optimized version of the nanostar small-angle X-ray scattering camera for solution scattering, J Appl Crystall 37 (2004) 369–380.
[22] G. Pabst, M. Rappolt, H. Amenitsch, P. Laggner, Structural information from multilamellar liposomes at full hydration: full q-range fitting with high quality X-ray data, Phys Rev E 62 (2000) 4000–4009.
[23] A. Caillé, Remarks on the scattering of X-rays by A-type smectics, C R Seances Acad Sci Ser B 274 (1972) 891–893.
[24] R. Zhang, R.M. Suter, J.F. Nagle, Theory of the structure factor of lipid bilayers, Phys Rev E 50 (1994) 5047–5060.
[25] J.S. Pedersen, Analysis of small-angle scattering data from colloids and polymer solutions: modeling and least-squares fitting, Adv Colloid Interface Sci 70 (1997) 171–210.
[26] J.S. Pedersen, D. Posselt, K. Mortensen, Analytical treatment of the resolution function for small-angle scattering, J Appl Crystall 23 (1990) 321–333.
[27] J.S. Pedersen, Resolution effects and analysis of small-angle neutron scattering data, J Physique IV 3 (1993) 491–498.
[28] R. Development, Core Team, R: A Language and Environment for Statistical Computing, R Foundation for Statistical Computing, Vienna, Austria3-900051-07-0, 2005.
[29] L.A. Bagatolli, E. Gratton, Two photon fluorescence microscopy of coexisting lipid domains in giant unilamellar vesicles of binary phospholipid mixtures, Biophys J 78 (2000) 290–305.
[30] Y. Higashino, A. Matsui, K. Ohki, Membrane fusion between liposomes composed of acidic phospholipids and neutral phospholipids induced by melittin: a differential scanning calorimetric study, J Biochem 130 (2001) 393–397.
[31] W. Curatolo, B. Sears, L. Neuringer, A calorimetry and deuterium NMR study of mixed model membranes of 1-palmitoyl-2-oleylphosphatidylcholine and saturated phosphatidylcholines, Biochim Biophys Acta 817 (1985) 261–270.
[32] S. Leibler, Curvature instability in membranes, J Physique 47 (1986) 507–516.
[33] A. Yeung, E. Evans, Unexpected dynamics in shape fluctuations of bilayer vesicles, J Phys II France 5 (1995) 1501–1523.

[34] T. Pott, P. Méléard, The dynamics of vesicle thermal fluctuations is controlled by intermonolayer friction, Europhys Lett 59 (2002) 87–93.
[35] W. Helfrich, Z. Naturforsch. 33 (1978).
[36] T. Sata, R.J. Havel, A.L. Jones, Characterization of subfractions of triglyceride-rich lipoproteins separated by gel chromatography from blood plasma of normolipemic and hyperlipemic humans, J Lipid Res 13 (1972) 757–768.
[37] K. Tauchi-Sato, S. Ozeki, T. Houjou, R. Taguchi, T. Fujimoto, The surface of lipid droplets is a phospholipid monolayer with a unique fatty acid composition, J Biol Chem 277 (2002) 44507–44512.
[38] P. Boström, L. Andersson, M. Rutberg, J. Perman, U. Lidberg, B.R. Johansson, J. Fernandez-Rodriguez, J. Ericson, T. Nilsson, J. BorŽn, S.-O. Olofsson, Snare proteins mediate fusion between cytosolic lipid droplets and are implicated in insulin sensitivity, Nat Cell Biol 9 (2007) 1286–1293.
[39] J.A. Napier, A.K. Stobart, P.R. Shewry, The structure and biogenesis of plant oil bodies: the role of the er membrane and the oleosin class of proteins, Plant Mol Biol 31 (1996) 945–956.
[40] Y. Ohsaki, J. Cheng, M. Suzuki, Y. Shinohara, A. Fujita, T. Fujimoto, Biogenesis of cytoplasmic lipid droplets: from the lipid ester globule in the membrane to the visible structure, Biochim Biophys Acta 1791 (2009) 399–407.
[41] J. Brotherus, O. Renkonen, Subcellular distributions of lipids in cultured bhk cells: evidence for the enrichment of lysobisphosphatidic acid and neutral lipids in lysosomes, J Lipid Res 18 (1977) 191–202.
[42] T. Kobayashi, E. Stang, K.S. Fang, P. de Moerloose, R.G. Parton, J. Gruenberg, A lipid associated with the antiphospholipid syndrome regulates endosome structure and function, Nature 392 (1998) 193–197.
[43] J. Ruiz, B. Ochoa, Quantification in the subnanomolar range of phospholipids and neutral lipids by monodimensional thin-layer chromatography and image analysis, J Lipid Res 38 (1997) 1482–1489.
[44] J. Heeren, W. Weber, U. Beisiegel, Intracellular processing of endocytosed triglyceride-rich lipoproteins comprises both recycling and degradation, J Cell Sci 112 (Pt 3) (1999) 349–359.
[45] K.T. W., H. C.M., Membranes of mammary gland. VI. Lipid and protein composition of golgi apparatus and rough endoplasmic reticulum from bovine mammary gland, J Dairy Sci 55 (1972) 1577–1585.
[46] W.B. Mackinnon, M. Dyne, K.T. Holmes, C.E. Mountford, R.S. Gupta, Further evidence that the narrow 1H magnetic resonance signals from malignant cells do not arise from intracellular lipid droplets, NMR Biomed 2 (1989) 161–164.
[47] A. Ferretti, A. Knijn, C. Raggi, M. Sargiacomo, High-resolution proton NMR measures mobile lipids associated with triton-resistant membrane domains in haematopoietic K562 cells lacking or expressing caveolin-1, Eur Biophys J 32 (2003) 83–95.
[48] L.C. Wright, J.T. Djordjevic, S.D. Schibeci, U. Himmelreich, N. Muljadi, P. Williamson, G.W. Lynch, Detergent-resistant membrane fractions contribute to the total 1H NMR-visible lipid signal in cells, Eur J Biochem 270 (2003) 2091–2100.
[49] C. Rémy, N. Fouilhé, I. Barba, E. Sam-Lal, H. Lahrech, M.-G. Cucurella, M. Izquierdo, A. Moreno, A. Ziegler, R. Massarelli, M. Décorps, C. Arús, Evidence that mobile lipids detected in rat brain glioma by 1H nuclear magnetic resonance correspond to lipid droplets, Cancer Res 57 (1997) 407–414.
[50] I. Barba, M.E. Cabanãs, C. Arús, The relationship between nuclear magnetic resonance-visible lipids, lipid droplets, and cell proliferation in cultured C6 cells, Cancer Res 59 (1999) 1861–1868.
[51] J.M. Hakumäki, R.A. Kauppinen, ^{1}H NMR visible lipids in the life and death of cells, Trends Biochem Sci 25 (2000) 357–362.
[52] Y. Pérez, H. Lahrech, M.E. Cabanãs, R. Barnadas, M. Sabés, C. Rémy, C. Arús, Measurement by nuclear magnetic resonance diffusion of the dimensions of the mobile lipid compartment in C6 cells, Cancer Res 62 (2002) 5672–5677.
[53] J.T. Mandeville, M.A. Lawson, F.R. Maxfield, Dynamic imaging of neutrophil migration in three dimensions: mechanical interactions between cells and matrix, J Leukoc Biol 61 (1997) 188–200.
[54] K. Wolf, R. Müller, S. Borgmann, E.-B. Bröcker, P. Friedl, Amoeboid shape change and contact guidance: T-lymphocyte crawling through fibrillar collagen is independent of matrix remodeling by MMPs and other proteases, Blood 102 (2003) 3262–3269.
[55] C.E. Mountford, G. Grossman, G. Reid, R.M. Fox, Characterization of transformed cells and tumors by proton nuclear magnetic resonance spectroscopy, Cancer Res 42 (1982) 2270–2276.
[56] P. Friedl, K. Wolf, Tumour-cell invasion and migration: diversity and escape mechanisms, Nat Rev Cancer 3 (2003) 362–374.
[57] G. Poste, G.L. Nicolson, Arrest and metastasis of blood-borne tumor cells are modified by fusion of plasma membrane vesicles from highly metastatic cell, Proc Nat Acad Sci USA 77 (1980) 399–403.
[58] K.T. Holmes, P.G. Williams, G.L. May, P. Gregory, L.C. Wright, M. Dyne, C.E. Mountford, Cell surface involvement in cancer metastasis: an NMR study, FEBS Lett 202 (1986) 122–126.
[59] L.C. Wright, G.L. May, M. Dyne, C.E. Mountford, A proteolipid in cancer cells is the origin of their high-resolution NMR spectrum, FEBS Lett 203 (1986) 164–168.
[60] T.D. Pollard, The cytoskeleton, cellular motility and the reductionist agenda, Nature 422 (2003) 741–745.